AIP Journal of Applied Physics

Observation of the large magnetocaloric effect and suppression of orbital entropy change in Fe-doped MnV2O4

Z. H. Huang, X. Luo, L. Hu, S. G. Tan, Y. Liu, B. Yuan, J. Chen, W. H. Song, and Y. P. Sun

Citation: Journal of Applied Physics **115**, 034903 (2014); doi: 10.1063/1.4861630
View online: http://dx.doi.org/10.1063/1.4861630
View Table of Contents: http://scitation.aip.org/content/aip/journal/jap/115/3?ver=pdfcov
Published by the AIP Publishing

Observation of the large magnetocaloric effect and suppression of orbital entropy change in Fe-doped MnV_2O_4

Z. H. Huang,[1] X. Luo,[2,a)] L. Hu,[2] S. G. Tan,[2] Y. Liu,[2] B. Yuan,[2] J. Chen,[2] W. H. Song,[2] and Y. P. Sun[1,2,a)]

[1]*High Magnetic Field Laboratory, Chinese Academy of Sciences, Hefei 230031, People's Republic of China*
[2]*Key Laboratory of Materials Physics, Institute of Solid State Physics, Chinese Academy of Sciences, Hefei 230031, People's Republic of China and University of Science and Technology of China, Hefei 230026, People's Republic of China*

(Received 17 October 2013; accepted 22 December 2013; published online 15 January 2014)

We present the structural and magnetic properties of $Mn_{1-x}Fe_xV_2O_4$ ($x = 0.1$, 0.2, and 0.3), and investigate the magnetocaloric effect in those compounds. The ferrimagnetic spin ordering is enhanced with the Fe doping at Mn site of MnV_2O_4, while the orbital ordering is suppressed. Large magnetic entropy changes up to 3.8 J/kg K as well as the relative cooling power up to 110 J/kg at the field change of 0-2 T for $Mn_{1-x}Fe_xV_2O_4$ are calculated from the isothermal magnetization measurements. The large orbital entropy change of MnV_2O_4 is suppressed by the Fe doping, while the spin entropy contribution arising from the strong spin-orbit coupling remains. Moreover, the doping of Fe broadens the temperature span of the large magnetic entropy change and increases the relative cooling power of MnV_2O_4 by 2.4 times. © *2014 AIP Publishing LLC*.
[http://dx.doi.org/10.1063/1.4861630]

I. INTRODUCTION AND EXPERIMENTAL DETAILS

Magnetic materials with large magnetocaloric effect (MCE) have attracted much interest due to their potential application for magnetic refrigeration technology. The key problem for the application of magnetic refrigeration technology is to search appropriate materials with large magnetic entropy change in wide temperature ranges. And one of the criteria for selecting magnetic refrigerators is the large MCE located in the temperature span of 10–80 K or >250 K.[1] Large MCEs are generally found in rare-earth materials and their alloys, for example, $ErMn_2Si_2$, $Eu_8Ga_{16}Ge_{30}$, HoCuSi, $ErRu_2Si_2$, Er_4NiCd, $PrCo_2B_2$, $Dy_{0.9}Tm_{0.1}Ni_2B_2C$, $GdCo_2B_2$, $La_{0.62}Bi_{0.05}Ca_{0.33}MnO_3$,[2–10] because of their large magnetic moments. However, the exorbitant price of the rare-earth materials is an inevitable limitation for the large-scale application of the magnetic refrigerator. Recently, large MCEs comparable with the rare-earth materials have been found in MnV_2O_4 and its Zn, Al doped compounds.[11–13] And their MCEs are located in the temperature range of 50 K-70 K, which is within the span of the low-temperature magnetic refrigerator. Moreover, the cost of the raw materials to synthesize MnV_2O_4 is much lower than that of traditional rare-earth MCE materials. Considering the above advantages, MnV_2O_4 has the potential application in low temperature magnetic refrigeration technology.

In addition, the spinel vanadium oxides, with the general formula AV_2O_4 (A = Zn, Mn, Fe, Co, Mg, and Cd), have many intriguing physical properties.[14–18] These compounds display complex behavior including structural transitions from cubic to tetragonal symmetries as well as complicated magnetic transitions. MnV_2O_4 is a typical example which exhibits a paramagnetic-ferrimagnetic transition (PM-FIM) at 57 K and a structural phase transition accompanied with t_{2g} orbital ordering (OO) at 53 K.[19,20] The giant MCE caused by the large orbital entropy of the t_{2g} OO transition was reported in our previous work on MnV_2O_4 and the minimal Zn-doped vanadate $Mn_{0.95}Zn_{0.05}V_2O_4$.[11,12] The magnetic entropy of MnV_2O_4 is very large but the temperature range of the large entropy is quite narrow. It is known that the magnetic entropy of MnV_2O_4 is mainly attributed to the change of the orbital state of V^{3+} ions.[11] The OO transition of MnV_2O_4 is quite sharp, which leads to the narrow temperature span of the orbital entropy. Furthermore, the Curie temperature is very close to the OO transition, which produces the close integration of the spin and orbital entropy and the narrow temperature range of the total magnetic entropy and there is obviously thermal hysteresis around the OO phase transition.

It is known that the orbital angular momentum of Mn^{2+} ($3d^5$) and Zn^{2+} ($3d^{10}$) ions are quenched but the Fe^{2+} ($3d^6$) ions in FeV_2O_4 still retain the orbital degrees of freedom and e_g orbital ordering in low temperature.[21] The Fe^{2+} ions substitution for Mn ones of MnV_2O_4 may influence the spin and orbital ordering, thereby, tune the magnetic entropy and the magnetic refrigerating capacity of MnV_2O_4. In this paper, we synthesize Fe^{2+} doped MnV_2O_4 polycrystalline samples and detailedly study the magnetization and magnetic entropy of the series samples $Mn_{1-x}Fe_xV_2O_4$ ($x = 0.1$, 0.2, and 0.3).

Polycrystalline samples of $Mn_{1-x}Fe_xV_2O_4$ ($x = 0.1$, 0.2, and 0.3) were synthesized by solid-state method. Stoichiometric mixtures of MnO, Fe, Fe_2O_3, and V_2O_3 were carefully grounded and pressed into pellets. These pellets were placed in Pt crucibles and sealed into evacuated quartz tubes. After being presintered at 973 K with 20 h, these pellets were grounded and pressed again and heated to 1223 K

a)Authors to whom correspondence should be addressed. Electronic addresses: xluo@issp.ac.cn and ypsun@issp.ac.cn. Tel.: +86-551-6559-2757. Fax: +86-551-6559-1434.

for 40 h in evacuated quartz tubes. The phase purity was examined by powder X-ray diffraction (XRD) using Cu-Ka radiation at room temperature. The Rietveld refinements were carried out using the program RIETICA. The magnetization measurements were performed with a Quantum Design (QD) Superconducting Quantum Interference Device (SQUID) system ($1.9 \leq T \leq 400$ K, $0 \leq H \leq 5$ T). The specific heat data were collected with a QD Physical Property Measurement System (PPMS) ($1.8 \leq T \leq 400$ K, $0 \leq H \leq 9$ T).

II. RESULTS AND DISCUSSIONS

The powder XRD patterns and the corresponding Rietveld analysis patterns of $Mn_{1-x}Fe_xV_2O_4$ at room temperature are displayed in Fig. 1(a) with 2θ scanning from 20° to 80°. All diffraction peaks can be indexed into a normal spinel structure, as shown in the Fig. 1(b), with the space group $Fd\bar{3}m$. The variation of lattice parameters (a) obtained from Rietveld analyses for $Mn_{1-x}Fe_xV_2O_4$ is shown in Fig. 1(c). With substitution of Fe for Mn ions, the lattice parameters of $Mn_{1-x}Fe_xV_2O_4$ show a linear decrease for x changing from 0.1 to 0.3. This decrease is consistent with the fact that ionic radius of Fe^{2+} ions (0.77 Å) is smaller than that of Mn^{2+} ions (0.80 Å). Diffraction peaks of impurity phase (Fe and Fe_2O_3) were found in the XRD patterns for $x = 0.35$ and 0.4, therefore, the Fe solubility limit in MnV_2O_4 is likely to lie between 30%–35% in the polycrystalline samples prepared with our preparation method.

Figure 2 shows the temperature dependence curves of the magnetization (M) for $Mn_{1-x}Fe_xV_2O_4$, which were measured at an external magnetic field of $H = 0.01$ T in the zero-field-cooled (ZFC), field-cooled cooling (FCC), and field-cooled warming (FCW) sequences. The FIM transition temperatures (T_C) are determined by the maximum slopes of the ZFC curves, and the temperatures of structural transition accompanied with t_{2g} orbital ordering (T_{oo}) are determined by the anomalies with thermal hysteresis between FCW and FCC curves at lower temperatures. In order to confirm the phase transition temperatures T_C and T_{oo} of $Mn_{1-x}Fe_xV_2O_4$, $Mn_{0.9}Fe_{0.1}V_2O_4$ was selected to perform the specific heat measurement. As shown in Fig. 2(a), the specific heat of $Mn_{0.9}Fe_{0.1}V_2O_4$ was measured without applied magnetic field in the cooling and warming processes. A λ-shaped heat-capacity anomaly without thermal hysteresis between cooling and warming sequences appears at the temperature of T_C, while a sharp and symmetrical peak with obvious thermal hysteresis is observed at the temperature of T_{oo}. The thermal hysteresis comes from the latent heat of the first-order phase transition, which is corresponding to the structural transition in this situation. It is found that the T_C shifts towards higher temperatures with the higher Fe doping, while T_{oo} shifts towards lower temperatures. In another

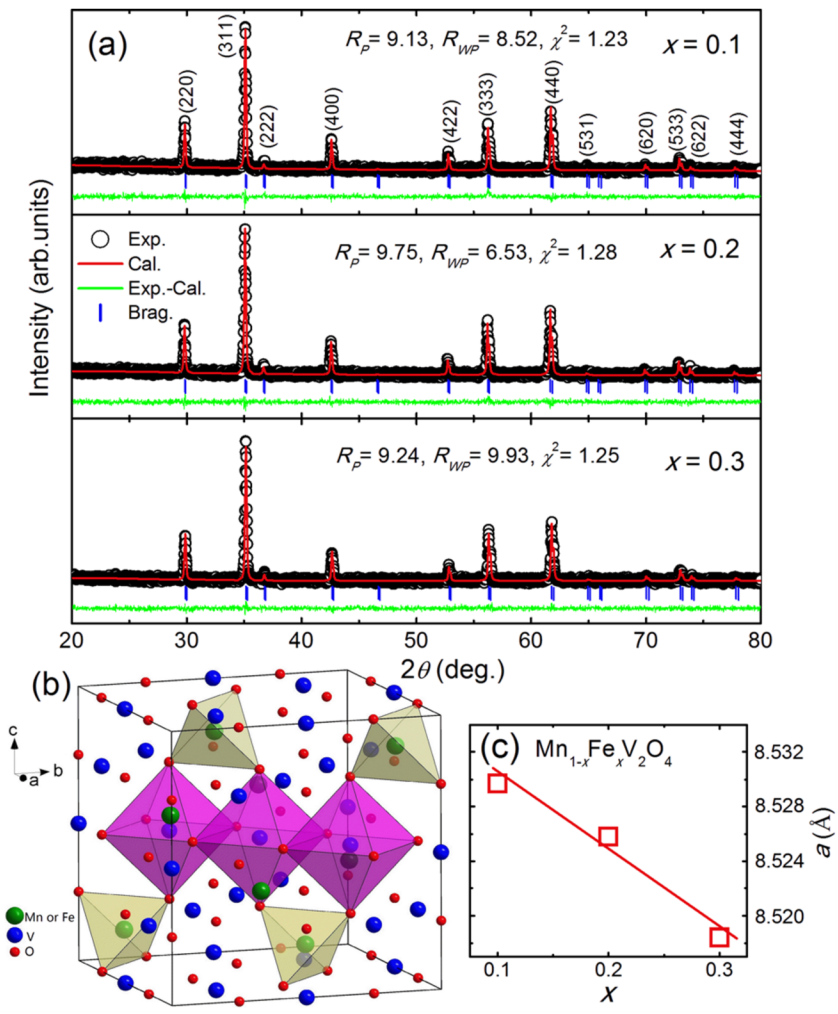

FIG. 1. (a) The X-ray powder diffraction patterns (circles) and Rietveld refinement (red solid curve) as well as the refinement parameters R_p, R_{wp}, and χ^2 for $Mn_{1-x}Fe_xV_2O_4$ at room temperature, the vertical marks symbolize the position of Bragg diffraction peaks, and the solid line at the bottom of diagram corresponds to the difference between the observed and calculated intensities. (b) The crystal structure of $Mn_{1-x}Fe_xV_2O_4$, the tetrahedrons and octahedrons represent the tetrahedral sites and octahedral sites. (c) The lattice parameters of different Fe content compounds at room temperature.

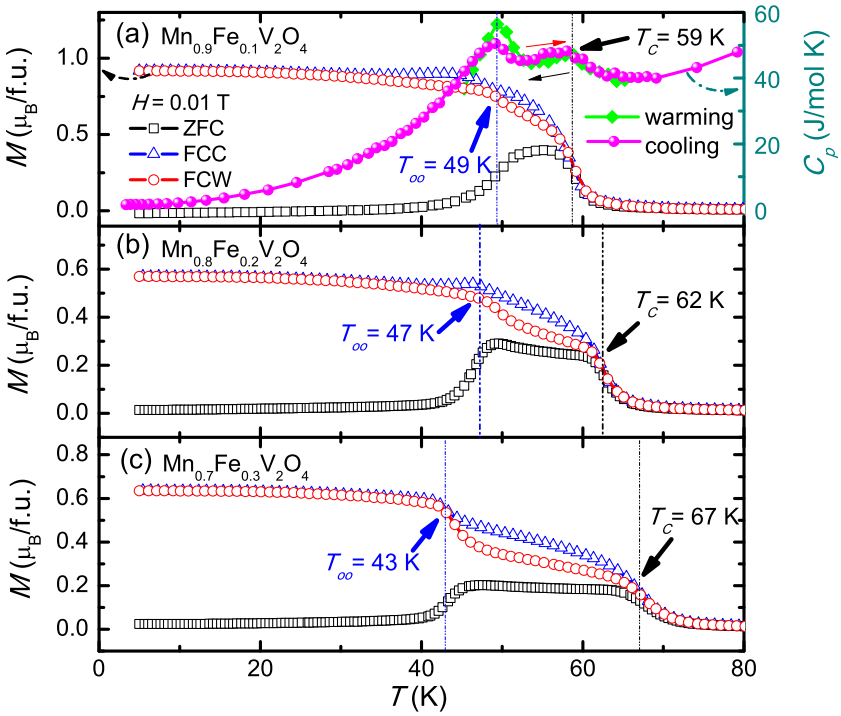

FIG. 2. The temperature dependence of: (a)–(c) magnetization (M) for $Mn_{1-x}Fe_xV_2O_4$ ($x = 0.1$, 0.2, and 0.3) at an external magnetic field $H = 0.01$ T (curves with hollow symbols); (a) the specific heat of $Mn_{0.9}Fe_{0.1}V_2O_4$ without a magnetic field (curves with solid symbols).

word, the FIM spin ordering is enhanced, while the OO is suppressed with the Fe doping at the Mn site of MnV_2O_4. The enhanced spin ordering is probably attributed to the lattice contraction caused by the Fe doping. And the mechanism of the suppressed OO by the Fe doping still needs further investigation.

Figure 3 shows the isothermal magnetization curves and the corresponding Arrott plots of $Mn_{1-x}Fe_xV_2O_4$ ($x = 0.1$, 0.2, and 0.3) in the temperature range of 30-90 K at the magnetic field up to 4.5 T. According to the previous studies,[22,23] the negative slope of Arrott plot indicates a first-order magnetic transition, such as a magnetostrictive transition. In contrast, a positive slope of Arrott plot implies a second-order magnetic transition. Herein, no negative slope is observed in the Arrott plots of $Mn_{1-x}Fe_xV_2O_4$, which confirms the second-order magnetic transitions in $Mn_{1-x}Fe_xV_2O_4$. Note that the MCE materials with second-order magnetic transitions have an advantage over the MCE materials with first-order magnetic transitions for the low hysteresis in both magnetic and thermal cycles.[24] The magnetic entropy change (ΔS_M) can be calculated from the Maxwell relation,

$$\Delta S_M(T,H) = S_M(T,H) - S_M(T,0) = \int_0^H \left(\frac{\partial M}{\partial T}\right)_H dH, \quad (1)$$

which can be converted into the formula,

$$\Delta S_M = \frac{1}{T_i - T_{i+1}} \sum_j (M_i - M_{i+1})_{H_j} \Delta H_j, \quad (2)$$

where the M_i is the magnetization at temperature T_i under magnetic field of H_j. ΔH_j is the increment of the external magnetic field.

The temperature dependences of $-\Delta S_M$ evaluated by Eq. (2) from the data of the isothermal magnetization curves are shown in Fig. 4. Two peaks are observed in each $-\Delta S_M$ *vs* T curve of three Fe-doped compounds. It is found that the two peak temperatures consist with the two phase transition temperature T_C and T_{oo}, respectively, where the $-\Delta S_M$ at T_{oo} is lower than $-\Delta S_M$ at T_C. It seems that both of these two transitions contribute to the $-\Delta S_M$. And it is observed that, with the raising applied magnetic fields, the $-\Delta S_M$ peaks at T_C obviously move to higher temperatures, while the position of the peaks at T_{oo} is nearly unchanged. According to the mean field theory, the ΔS_M *vs* H at the magnetic phase transition T_C shows the 2/3 power law dependence,[25]

$$\Delta S_M \approx -1.07qR\left(\frac{g\mu_B JH}{kT_C}\right)^{2/3}, \quad (3)$$

where q represent the number of magnetic ions per mole, R is the gas constant, and g the Laudé factor. The relationship

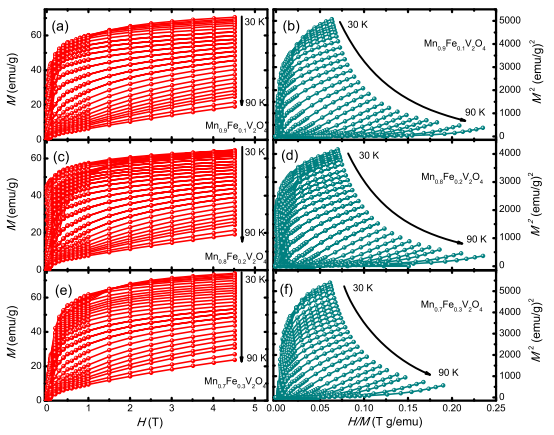

FIG. 3. (a), (c), (e) The isothermal magnetization curves and (b), (d), (f) their corresponding Arrott plots of $Mn_{1-x}Fe_xV_2O_4$ ($x = 0.1$, 0.2, and 0.3) in the temperature range of 30-90 K at the magnetic field up to 4.5 T.

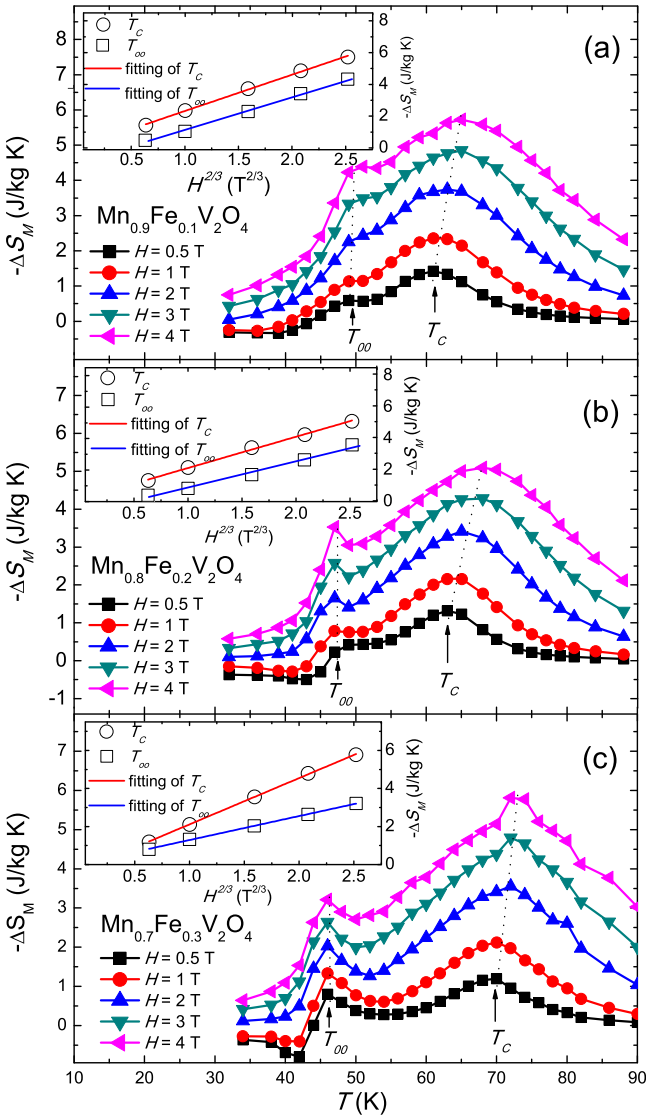

FIG. 4. (a)–(c) Entropy changes of $Mn_{1-x}Fe_xV_2O_4$ ($x = 0.1$, 0.2, and 0.3) extracted from isothermal magnetization measurements with the magnetic field changes from 0 to 0.5 T, 1 T, 2 T, 3 T, and 4 T. The insets display the relation between $-\Delta S_M^{max}$ and $H^{2/3}$ near the T_C and T_{oo}. The straight lines represent the linear fitting of that relation.

between the maximum $-\Delta S_M$ and $H^{2/3}$ around T_C and T_{oo} are plotted in the inset of Fig. 4 to confirm the 2/3 power dependence of $-\Delta S_M$ *vs* H. It is found that the $-\Delta S_M$ displays well linear relationship with $H^{2/3}$ at T_C and T_{oo} for all three compounds. It is reported that the $-\Delta S_M$ of MnV_2O_4 is mainly ascribed to the orbital entropy change of V^{3+} ions induced by the magnetic field, therefore, the maximum $-\Delta S_M$ of MnV_2O_4 deviates from the linear dependence with $H^{2/3}$.[11] The linear dependences of $-\Delta S_M$ *vs* $H^{2/3}$ around T_{oo} of these Fe-doped compounds indicate that the orbital entropy changes are suppressed and the $-\Delta S_M$ at T_{oo} are mainly attributed to the spin entropy contribution due to the strong spin-orbit coupling. In addition, the $-\Delta S_M$ at T_{oo} of about 2 J/kg K at field change of 0-2 T in the Fe-doped compounds is much lower than the orbital entropy change of 14.8 J/kg K at the same field change in MnV_2O_4,[11] that further demonstrates the suppression of the orbital entropy changes by the Fe doping at the Mn site of MnV_2O_4.

The relative cooling power (RCP) is another important parameter for evaluating the magnetic refrigeration capacity. The RCP value represents the maximum thermal energy that can be transferred in one refrigeration cycle.[26] The RCP is defined as

$$\mathrm{RCP} = \int -\Delta S_M dT. \tag{4}$$

After the integrations of the $-\Delta S_M$ *vs* T curves in Fig. 4, the magnetic transition temperature (T_M), the maximum value of the magnetic entropy change ($-\Delta S_M^{max}$), and the RCP value of $Mn_{1-x}Fe_xV_2O_4$ ($x = 0.1$, 0.2, and 0.3) at the magnetic field change of 2 T are represented in Fig. 5 as well as some other giant MCE materials, such as MnV_2O_4, $MnV_{1.95}Al_{0.05}O_4$, $CdCr_2S_4$,[27] $ErMn_2Si_2$, $Eu_8Ga_{16}Ge_{30}$, HoCuSi, $ErRu_2Si_2$, Er_4NiCd, $PrCo_2B_2$, $Dy_{0.9}Tm_{0.1}Ni_2B_2C$, $GdCo_2B_2$, $La_{0.62}Bi_{0.05}Ca_{0.33}MnO_3$.[2–9] It is found that the $-\Delta S_M^{max}$ values of $Mn_{1-x}Fe_xV_2O_4$ are less than other MCE materials, but their RCP values are much higher than many of others. It is indicated that the large RCP values of $Mn_{1-x}Fe_xV_2O_4$ come from the wide temperature ranges of the magnetic entropy change. As we discussed above, the doping of Fe in MnV_2O_4 leads to the higher T_C and lower T_{oo} (the phase transitions of MnV_2O_4 are $T_C = 57$ K and $T_{oo} = 53$ K),[11,19,20] which broaden the temperature spans of the magnetic entropy change. Compared with pure MnV_2O_4, the RCP values of Fe-doped compounds are greatly improved (the RCP values at the field change of 0–2 T are 46.7 J/kg for MnV_2O_4 and up to 110 J/kg for the Fe-doped compounds). Therefore, the Fe doped MnV_2O_4 is probably a promising candidate as a working material below 80 K for magnetic refrigeration technology.

In summary, the $Mn_{1-x}Fe_xV_2O_4$ ($x = 0.1$, 0.2, and 0.3) display large magnetic entropy changes in wide temperature ranges, which are attributed to the FIM transition and the

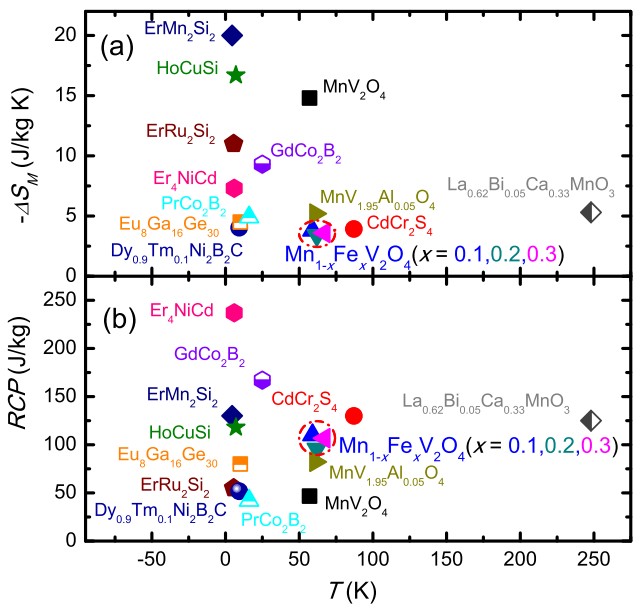

FIG. 5. The comparison of (a) $-\Delta S_M^{max}$ and (b) RCP values of $Mn_{1-x}Fe_xV_2O_4$ ($x = 0.1$, 0.2, and 0.3) with other giant MCE materials at the magnetic field change of 0-2T. The red dashed circles are guide to the eye.

OO transition. The T_C phase transition is enhanced and the T_{oo} is suppressed for $Mn_{1-x}Fe_xV_2O_4$. In the Fe-doped compounds, the orbital entropy changes are suppressed and the $-\Delta S_M$ at T_{oo} is mainly attributed to the spin entropy contribution due to the strong spin-orbit coupling. And the magnetic refrigerant capacities of $Mn_{1-x}Fe_xV_2O_4$ are much larger than many other MCE materials including MnV_2O_4 because of the wide temperature spans of $-\Delta S_M$, which are broadened by the shift of the T_C and T_{oo}.

ACKNOWLEDGMENTS

This work was supported by the National Nature Science Foundation of China under Contract Nos. 11004193, 10974205, and 11104273 and the Knowledge Innovation Program of the Chinese Academy of Sciences under Contract No. Y04N371121.

[1]M. H. Phan and S. C. Yu, J. Magn. Magn. Mater. **308**, 325–340 (2007).
[2]L. W. Li, K. Nishimura, W. D. Hutchison, Z. H. Qian, D. X. Huo, and T. Namiki, Appl. Phys. Lett. **100**, 152403 (2012).
[3]A. Chaturvedi, S. Stefanoski, M. H. Phan, G. S. Nolas, and H. Srikanth, Appl. Phys. Lett. **99**, 162513 (2011).
[4]J. Chen, B. G. Shen, Q. Y. Dong, F. X. Hu, and J. R. Sun, Appl. Phys. Lett. **96**, 152501 (2010).
[5]T. Samanta, I. Das, and S. Banerjee, Appl. Phys. Lett. **91**, 152506 (2007).
[6]W. Hermes, U. Ch. Rodewals, and R. Pottgen, J. Appl. Phys. **108**, 113919 (2010).
[7]L. Li and K. Nishimura, J. Appl. Phys. **106**, 023903 (2009).
[8]L. Li and K. Nishimura, Appl. Phys. Lett. **95**, 132505 (2009).
[9]L. Li, K. Nishimura, and H. Yamane, Appl. Phys. Lett. **94**, 102509 (2009).
[10]H. Gencer, S. Atalay, H. I. Adiguzel, and V. S. Kolat, Physica B **357**, 326 (2005).
[11]X. Luo, Y. P. Sun, L. Hu, B. S. Wang, W. J. Lu, X. B. Zhu, Z. R. Yang, and W. H. Song, J. Phys.: Condens. Matter **21**, 436010 (2009).
[12]X. Luo, Y. P. Sun, W. J. Lu, X. B. Zhu, Z. R. Yang, and W. H. Song, Appl. Phys. Lett. **96**, 062506 (2010).
[13]X. Luo, W. J. Lu, Z. H. Huang, X. B. Hu, L. Hu, X. B. Zhu, Z. R. Yang, W. H. Song, J. M. Dai, and Y. P. Sun, J. Magn. Magn. Mater. **324**, 766 (2012).
[14]K. Adachi, T. Suzuki, K. Kato, K. Osaka, M. Takata, and T. Katsufuji, Phys. Rev. Lett. **95**, 197202 (2005).
[15]P. G. Radaelli, New J. Phys. **7**, 53 (2005).
[16]Y. Nii, H. Sagayama, T. Arima, S. Aoyagi, R. Sakai, S. Maki, E. Nishibori, H. Sawa, K. Sugimoto, H. Ohsumo, and M. Takata, Phys. Rev. B **86**, 125142 (2012).
[17]A. Kismarahardja, J. S. Brooks, A. Kiswandhi, K. Matsubayashi, R. Yamanaka, Y. Uwatoko, J. Whalen, T. Siegrist, and H. D. Zhou, Phys. Rev. Lett. **106**, 056602 (2011).
[18]D. Baldomir, V. Pardo, S. Blanco-Canosa, F. Rivadulla, J. Rivas, A. Pineiro, and J. E. Arias, Physica B **403**, 1639 (2008).
[19]H. D. Zhou, J. Lu, and C. R. Wiebe, Phys. Rev. B **76**, 174403 (2007).
[20]T. Suzuki, M. Katsumura, K. Taniguchi, T. Arima, and T. Katsufuji, Phys. Rev. Lett. **98**, 127203 (2007).
[21]T. Katsufuji, T. Suzuki, H. Takei, M. Shingu, K. Kato, K. Osaka, and M. Takata, J. Phys. Soc. Jpn. **77**, 053708 (2008).
[22]B. K. Banerjee, Phys. Lett. **12**, 16 (1964).
[23]Y. D. Zhang, P. J. Lampen, T.-L. Phan, S.-C. Yu, H. Srikanth, and M.-H. Phan, J. Appl. Phys. **111**, 063918 (2012).
[24]V. K. Pecharsky and K. A. Gschneider, Jr., J. Magn. Magn. Mater. **200**, 44 (1999).
[25]H. Oesterreicher and F. T. Parker, J. Appl. Phys. **55**, 4334 (1984).
[26]M. J. Shao, S. X. Cao, S. J. Yuan, J. Shang, B. J. Kang, B. Lu, and J. C. Zhang, Appl. Phys. Lett. **100**, 222404 (2012).
[27]L. Q. Yan, J. Shen, Y. X. Li, F. W. Wang, Z. W. Jiang, F. X. Hu, J. R. Sun, and B. G. Shen, Appl. Phys. Lett. **90**, 262502 (2007).